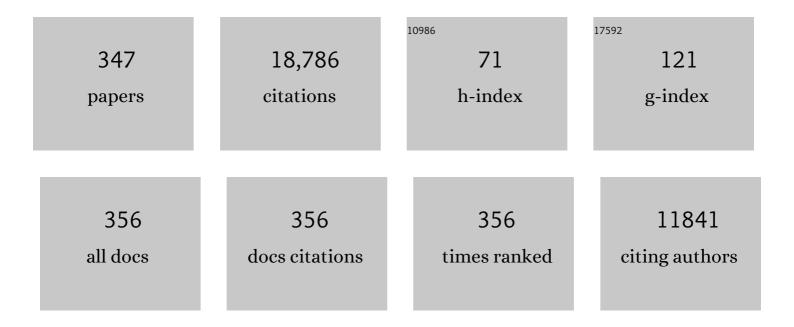
## Mitchell A Winnik

List of Publications by Year in descending order

Source: https://exaly.com/author-pdf/3675556/publications.pdf Version: 2024-02-01



#	Article	IF	CITATIONS
1	Cylindrical Block Copolymer Micelles and Co-Micelles of Controlled Length and Architecture. Science, 2007, 317, 644-647.	12.6	1,025
2	Monodisperse cylindrical micelles by crystallization-driven living self-assembly. Nature Chemistry, 2010, 2, 566-570.	13.6	537
3	Multidimensional hierarchical self-assembly of amphiphilic cylindrical block comicelles. Science, 2015, 347, 1329-1332.	12.6	443
4	THE P <i>y</i> SCALE OF SOLVENT POLARITIES. SOLVENT EFFECTS ON THE VIBRONIC FINE STRUCTURE OF PYRENE FLUORESCENCE and EMPIRICAL CORRELATIONS WITH <i>E</i> <sub>T</sub> and <i>Y</i> VALUES. Photochemistry and Photobiology, 1982, 35, 17-21.	2.5	439
5	Complex and hierarchical micelle architectures from diblock copolymers using living, crystallization-driven polymerizations. Nature Materials, 2009, 8, 144-150.	27.5	429
6	Self-Assembly of Organometallic Block Copolymers:  The Role of Crystallinity of the Core-Forming Polyferrocene Block in the Micellar Morphologies Formed by Poly(ferrocenylsilane-b-dimethylsiloxane) in n-Alkane Solvents. Journal of the American Chemical Society, 2000, 122, 11577-11584.	13.7	356
7	Non-Centrosymmetric Cylindrical Micelles by Unidirectional Growth. Science, 2012, 337, 559-562.	12.6	342
8	Tailored hierarchical micelle architectures using living crystallization-driven self-assembly in two dimensions. Nature Chemistry, 2014, 6, 893-898.	13.6	329
9	Highly multiparametric analysis by mass cytometry. Journal of Immunological Methods, 2010, 361, 1-20.	1.4	328
10	Uniform patchy and hollow rectangular platelet micelles from crystallizable polymer blends. Science, 2016, 352, 697-701.	12.6	305
11	Self-Assembly of a Novel Organometallicâ `Inorganic Block Copolymer in Solution and the Solid State:Â Nonintrusive Observation of Novel Wormlike Poly(ferrocenyldimethylsilane)-b-Poly(dimethylsiloxane) Micelles. Journal of the American Chemical Society, 1998, 120, 9533-9540.	13.7	303
12	Polymer-Based Elemental Tags for Sensitive Bioassays. Angewandte Chemie - International Edition, 2007, 46, 6111-6114.	13.8	247
13	Colour-tunable fluorescent multiblock micelles. Nature Communications, 2014, 5, 3372.	12.8	243
14	Cylindrical Micelles of Controlled Length with a π-Conjugated Polythiophene Core via Crystallization-Driven Self-Assembly. Journal of the American Chemical Society, 2011, 133, 8842-8845.	13.7	235
15	Latex film formation. Current Opinion in Colloid and Interface Science, 1997, 2, 192-199.	7.4	234
16	Structureâ€īuned Lead Halide Perovskite Nanocrystals. Advanced Materials, 2016, 28, 566-573.	21.0	215
17	Two-Stage Dispersion Polymerization toward Monodisperse, Controlled Micrometer-Sized Copolymer Particles. Journal of the American Chemical Society, 2004, 126, 6562-6563.	13.7	198
18	Influence of the Interplay of Crystallization and Chain Stretching on Micellar Morphologies:Â Solution Self-Assembly of Coilâ^'Crystalline Poly(isoprene-block-ferrocenylsilane). Macromolecules, 2002, 35, 8258-8260.	4.8	192

#	Article	IF	CITATIONS
19	Monodisperse Fiber-like Micelles of Controlled Length and Composition with an Oligo( <i>p</i> -phenylenevinylene) Core via "Living―Crystallization-Driven Self-Assembly. Journal of the American Chemical Society, 2017, 139, 7136-7139.	13.7	187
20	Uniform, High Aspect Ratio Fiber-like Micelles and Block Co-micelles with a Crystalline π-Conjugated Polythiophene Core by Self-Seeding. Journal of the American Chemical Society, 2014, 136, 4121-4124.	13.7	181
21	Two-dimensional assemblies from crystallizable homopolymers with charged termini. Nature Materials, 2017, 16, 481-488.	27.5	179
22	Molecular aspects of latex film formation: an energy-transfer study. Macromolecules, 1990, 23, 4082-4087.	4.8	168
23	Molecular diffusion and latex film formation: An analysis of direct nonradiative energy transfer experiments. Journal of Chemical Physics, 1991, 95, 2143-2153.	3.0	153
24	Cross-Linked, Monodisperse, Micron-Sized Polystyrene Particles by Two-Stage Dispersion Polymerization. Macromolecules, 2005, 38, 8300-8307.	4.8	151
25	Self‣eeding in One Dimension: An Approach To Control the Length of Fiberlike Polyisoprene–Polyferrocenylsilane Block Copolymer Micelles. Angewandte Chemie - International Edition, 2011, 50, 1622-1625.	13.8	141
26	Cylindrical Block Co-Micelles with Spatially Selective Functionalization by Nanoparticles. Journal of the American Chemical Society, 2007, 129, 12924-12925.	13.7	140
27	A Water-Soluble pH-Responsive Molecular Brush of Poly( <i>N</i> , <i>N</i> -dimethylaminoethyl) Tj ETQq1 1 0.7	84314 rgB <sup>-</sup> 4.8	Г /Qygrlock 1(
28	Nanofiber micelles from the self-assembly of block copolymers. Trends in Biotechnology, 2010, 28, 84-92.	9.3	132
29	Synthesis, Characterization, and Rheological Behavior of Polyethylene Glycols End-Capped with Fluorocarbon Hydrophobes. Langmuir, 1997, 13, 2447-2456.	3.5	130
30	Evolution of Selfâ€Assembled Structures of Polymerâ€Terminated Gold Nanorods in Selective Solvents. Advanced Materials, 2008, 20, 4318-4322.	21.0	124
31	Redox-Induced Synthesis and Encapsulation of Metal Nanoparticles in Shell-Cross-Linked Organometallic Nanotubes. Journal of the American Chemical Society, 2005, 127, 8924-8925.	13.7	120
32	Uniform electroactive fibre-like micelle nanowires for organic electronics. Nature Communications, 2017, 8, 15909.	12.8	120
33	Development of analytical methods for multiplex bio-assay with inductively coupled plasma mass spectrometry. Journal of Analytical Atomic Spectrometry, 2008, 23, 463.	3.0	115
34	Redox-Mediated Synthesis and Encapsulation of Inorganic Nanoparticles in Shell-Cross-Linked Cylindrical Polyferrocenylsilane Block Copolymer Micelles. Journal of the American Chemical Society, 2008, 130, 12921-12930.	13.7	115
35	Copolymerization propagation kinetics of styrene with alkyl acrylates. Polymer International, 1991, 24, 65-70.	3.1	113
36	Monodisperse Cylindrical Micelles of Controlled Length with a Liquidâ€Crystalline Perfluorinated Core by 1D "Selfâ€Seedingâ€: Angewandte Chemie - International Edition, 2016, 55, 11392-11396.	13.8	108

#	Article	IF	CITATIONS
37	Shell-Cross-Linked Cylindrical Polyisoprene-b-Polyferrocenylsilane (PI-b-PFS) Block Copolymer Micelles:Â One-Dimensional (1D) Organometallic Nanocylinders. Journal of the American Chemical Society, 2007, 129, 5630-5639.	13.7	105
38	Pointedâ€Ovalâ€Shaped Micelles from Crystallineâ€Coil Block Copolymers by Crystallizationâ€Driven Living Selfâ€Assembly. Angewandte Chemie - International Edition, 2010, 49, 8220-8223.	13.8	105
39	Synthesis of a Functional Metal-Chelating Polymer and Steps toward Quantitative Mass Cytometry Bioassays. Analytical Chemistry, 2010, 82, 8961-8969.	6.5	105
40	Fluorescent "Barcode―Multiblock Co-Micelles via the Living Self-Assembly of Di- and Triblock Copolymers with a Crystalline Core-Forming Metalloblock. Journal of the American Chemical Society, 2011, 133, 9095-9103.	13.7	102
41	Synthesis and Characterization of Pyrene-Labeled Poly(ethylenimine). Macromolecules, 1998, 31, 6855-6864.	4.8	101
42	Branched Micelles by Living Crystallization-Driven Block Copolymer Self-Assembly under Kinetic Control. Journal of the American Chemical Society, 2015, 137, 2375-2385.	13.7	101
43	Fabrication of Continuous and Segmented Polymer/Metal Oxide Nanowires Using Cylindrical Micelles and Block Comicelles as Templates. Advanced Materials, 2009, 21, 1805-1808.	21.0	99
44	Complex and Hierarchical 2D Assemblies via Crystallization-Driven Self-Assembly of Poly( <scp>l</scp> -lactide) Homopolymers with Charged Termini. Journal of the American Chemical Society, 2017, 139, 9221-9228.	13.7	99
45	Organometallic Nanostructures: Self-Assembly of Poly(ferrocene) Block Copolymers. Advanced Materials, 1998, 10, 1559-1562.	21.0	98
46	Self-Seeding in One Dimension: A Route to Uniform Fiber-like Nanostructures from Block Copolymers with a Crystallizable Core-Forming Block. ACS Nano, 2013, 7, 3754-3766.	14.6	98
47	Water-Soluble CdSe Quantum Dots Passivated by a Multidentate Diblock Copolymer. Macromolecules, 2007, 40, 6377-6384.	4.8	95
48	Fiber-like Micelles via the Crystallization-Driven Solution Self-Assembly of Poly(3-hexylthiophene)- <i>block</i> -Poly(methyl methacrylate) Copolymers. Macromolecules, 2012, 45, 5806-5815.	4.8	95
49	Multi-Armed Micelles and Block Co-micelles via Crystallization-Driven Self-Assembly with Homopolymer Nanocrystals as Initiators. Journal of the American Chemical Society, 2013, 135, 12180-12183.	13.7	94
50	Gradient Crystallization-Driven Self-Assembly: Cylindrical Micelles with "Patchy―Segmented Coronas via the Coassembly of Linear and Brush Block Copolymers. Journal of the American Chemical Society, 2014, 136, 13835-13844.	13.7	94
51	Crystallization-Driven Self-Assembly of Block Copolymers with a Short Crystallizable Core-Forming Segment: Controlling Micelle Morphology through the Influence of Molar Mass and Solvent Selectivity. Macromolecules, 2014, 47, 2361-2372.	4.8	93
52	Non-covalent synthesis of supermicelles with complex architectures using spatially confined hydrogen-bonding interactions. Nature Communications, 2015, 6, 8127.	12.8	93
53	Determination of propagation rate constants for the copolymerization of methymethacrylate and styrene using a pulsed laser technique. Journal of Polymer Science, Part C: Polymer Letters, 1989, 27, 181-185.	0.7	92
54	Synthesis and Self-Assembly of Poly(ferrocenyldimethylsilane-b-2-vinylpyridine) Diblock Copolymers. Macromolecules, 2007, 40, 3784-3789.	4.8	92

#	Article	IF	CITATIONS
55	Lanthanide-Containing Polymer Microspheres by Multiple-Stage Dispersion Polymerization for Highly Multiplexed Bioassays. Journal of the American Chemical Society, 2009, 131, 15276-15283.	13.7	92
56	Intratumorally Injected <sup>177</sup> Lu-Labeled Gold Nanoparticles: Gold Nanoseed Brachytherapy with Application for Neoadjuvant Treatment of Locally Advanced Breast Cancer. Journal of Nuclear Medicine, 2016, 57, 936-942.	5.0	92
57	Probing the Structure of the Crystalline Core of Field-Aligned, Monodisperse, Cylindrical Polyisoprene- <i>block</i> -Polyferrocenylsilane Micelles in Solution Using Synchrotron Small- and Wide-Angle X-ray Scattering. Journal of the American Chemical Society, 2011, 133, 17056-17062.	13.7	91
58	Dimensional Control of Block Copolymer Nanofibers with a ï€â€Conjugated Core: Crystallizationâ€Driven Solution Selfâ€Assembly of Amphiphilic Poly(3â€hexylthiophene)â€ <i>b</i> â€poly(2â€vinylpyridine). Chemistry - European Journal, 2013, 19, 9186-9197.	- A3.3	91
59	A Micellar Sphere-to-Cylinder Transition of Poly(ferrocenyldimethylsilane- <i>b</i> -2-vinylpyridine) in a Selective Solvent Driven by Crystallization. Macromolecules, 2008, 41, 4380-4389.	4.8	90
60	Monodisperse Cylindrical Micelles and Block Comicelles of Controlled Length in Aqueous Media. Journal of the American Chemical Society, 2016, 138, 4484-4493.	13.7	90
61	Shell Cross-Linked Cylinders of Polyisoprene-b-ferrocenyldimethylsilane:Â Formation of Magnetic Ceramic Replicas and Microfluidic Channel Alignment and Patterning. Journal of the American Chemical Society, 2003, 125, 12686-12687.	13.7	88
62	Effect of Water on Polymer Diffusion in Latex Films. Macromolecules, 1997, 30, 4324-4331.	4.8	87
63	Fluorescent Probe Studies of the Association in an Aqueous Solution of a Hydrophobically Modified Poly(ethylene oxide). Macromolecules, 1998, 31, 8998-9007.	4.8	84
64	Fragmentation of Fiberlike Structures: Sonication Studies of Cylindrical Block Copolymer Micelles and Behavioral Comparisons to Biological Fibrils. Journal of the American Chemical Society, 2008, 130, 14763-14771.	13.7	84
65	Functional latex and thermoset latex films. Journal of Coatings Technology Research, 2004, 1, 163-190.	2.5	83
66	Polymer/Silica Composite Films as Luminescent Oxygen Sensors. Macromolecules, 2001, 34, 1917-1927.	4.8	81
67	Lanthanide-Containing Polymer Nanoparticles for Biological Tagging Applications:  Nonspecific Endocytosis and Cell Adhesion. Journal of the American Chemical Society, 2007, 129, 13653-13660.	13.7	78
68	Uniform "Patchy―Platelets by Seeded Heteroepitaxial Growth of Crystallizable Polymer Blends in Two Dimensions. Journal of the American Chemical Society, 2017, 139, 4409-4417.	13.7	78
69	Reversible Cross-Linking of Polyisoprene Coronas in Micelles, Block Comicelles, and Hierarchical Micelle Architectures Using Pt(0)–Olefin Coordination. Journal of the American Chemical Society, 2011, 133, 16947-16957.	13.7	75
70	Flowable networks as DNA sequencing media in capillary columns. Electrophoresis, 1996, 17, 1451-1459.	2.4	74
71	A design strategy for the hierarchical fabrication of colloidal hybrid mesostructures. Nature Communications, 2014, 5, 3882.	12.8	73
72	Monodisperse Micrometer-Size Carboxyl-Functionalized Polystyrene Particles Obtained by Two-Stage Dispersion Polymerization. Macromolecules, 2006, 39, 5729-5737.	4.8	72

#	Article	IF	CITATIONS
73	Tunable Supermicelle Architectures from the Hierarchical Selfâ€Assembly of Amphiphilic Cylindrical B–A–B Triblock Coâ€Micelles. Angewandte Chemie - International Edition, 2012, 51, 11882-11885.	13.8	72
74	Effect of surface acid group neutralization on interdiffusion rates in latex films. Macromolecules, 1994, 27, 1007-1012.	4.8	71
75	Influence of Chain Length and Salt Concentration on Block Copolymer Micellization. Macromolecules, 1997, 30, 4911-4919.	4.8	70
76	Radiation Nanomedicine for EGFR-Positive Breast Cancer: Panitumumab-Modified Gold Nanoparticles Complexed to the β-Particle-Emitter, <sup>177</sup> Lu. Molecular Pharmaceutics, 2015, 12, 3963-3972.	4.6	67
77	Self-Seeding of Block Copolymers with a π-Conjugated Oligo( <i>p</i> -phenylenevinylene) Segment: A Versatile Route toward Monodisperse Fiber-like Nanostructures. Macromolecules, 2018, 51, 2065-2075.	4.8	67
78	Self-Assembled Organometallic Block Copolymer Nanotubes. Angewandte Chemie - International Edition, 2000, 39, 3862-3865.	13.8	66
79	Synthesis and Aqueous Self-Assembly of a Polyferrocenylsilane-block-poly(aminoalkyl methacrylate) Diblock Copolymer. Macromolecular Rapid Communications, 2002, 23, 210-213.	3.9	65
80	Light Scattering Study of Rigid, Rodlike Organometallic Block Copolymer Micelles in Dilute Solution. Macromolecules, 2005, 38, 7819-7827.	4.8	64
81	Crystallization-Driven Solution Self-Assembly of Block Copolymers with a Photocleavable Junction. Journal of the American Chemical Society, 2015, 137, 2203-2206.	13.7	64
82	Probing the Scope of Crystallization-Driven Living Self-Assembly: Studies of Diblock Copolymer Micelles with a Polyisoprene Corona and a Crystalline Poly(ferrocenyldiethylsilane) Core-Forming Metalloblock. Macromolecules, 2011, 44, 3777-3786.	4.8	63
83	Continuous and Segmented Semiconducting Fiberâ€like Nanostructures with Spatially Selective Functionalization by Living Crystallizationâ€Driven Selfâ€Assembly. Angewandte Chemie - International Edition, 2020, 59, 8232-8239.	13.8	63
84	Swellable, Redox-Active Shell-Crosslinked Organometallic Nanotubes. Angewandte Chemie - International Edition, 2004, 43, 3703-3707.	13.8	62
85	Hierarchical Assembly of Cylindrical Block Comicelles Mediated by Spatially Confined Hydrogen-Bonding Interactions. Journal of the American Chemical Society, 2016, 138, 12902-12912.	13.7	62
86	Study of polymer diffusion across the interface in latex films through direct energy transfer experiments. Journal of Chemical Physics, 1994, 101, 9096-9103.	3.0	61
87	Effect of Cross-Linking on Polymer Diffusion in Poly(butyl methacrylate-co-butyl acrylate) Latex Films. Macromolecules, 1999, 32, 6102-6110.	4.8	61
88	Solution Self-Assembly of Blends of Crystalline-Coil Polyferrocenylsilane- <i>block</i> -polyisoprene with Crystallizable Polyferrocenylsilane Homopolymer. Macromolecules, 2015, 48, 707-716.	4.8	61
89	Local Radiation Treatment of HER2-Positive Breast Cancer Using Trastuzumab-Modified Gold Nanoparticles Labeled with 177Lu. Pharmaceutical Research, 2017, 34, 579-590.	3.5	61
90	Probing the Growth Kinetics for the Formation of Uniform 1D Block Copolymer Nanoparticles by Living Crystallization-Driven Self-Assembly. ACS Nano, 2018, 12, 8920-8933.	14.6	60

#	Article	IF	CITATIONS
91	Branched Cylindrical Micelles via Crystallization-Driven Self-Assembly. Journal of the American Chemical Society, 2013, 135, 17739-17742.	13.7	59
92	Fluorescent polymer particles by emulsion and miniemulsion polymerization. Journal of Polymer Science Part A, 2003, 41, 766-778.	2.3	58
93	"Cross―Supermicelles via the Hierarchical Assembly of Amphiphilic Cylindrical Triblock Comicelles. Journal of the American Chemical Society, 2016, 138, 4087-4095.	13.7	58
94	Interaction of Pyrene-Labeled Poly(ethylene imine) with Sodium Dodecyl Sulfate in Aqueous Solution. Macromolecules, 1999, 32, 624-632.	4.8	55
95	Organometallicâ~'Polypeptide Block Copolymers:Â Synthesis and Properties of Poly(ferrocenyldimethylsilane)-b-poly- (l³-benzyl-l-glutamate). Macromolecules, 2005, 38, 4958-4961.	4.8	55
96	Influence of Solvent Polarity on the Self-Assembly of the Crystalline–Coil Diblock Copolymer Polyferrocenylsilane- <i>b</i> -polyisoprene. Macromolecules, 2011, 44, 6136-6144.	4.8	55
97	Surfactant exudation in the presence of a coalescing aid in latex films studied by atomic force microscopy1. Journal of Polymer Science, Part B: Polymer Physics, 1995, 33, 1123-1133.	2.1	53
98	Phosphorescent oxygen sensors utilizing sulfur-nitrogen-phosphorus polymer matrices. Advanced Materials, 1996, 8, 768-771.	21.0	53
99	End-to-End Coupling and Network Formation Behavior of Cylindrical Block Copolymer Micelles with a Crystalline Polyferrocenylsilane Core. Journal of the American Chemical Society, 2011, 133, 11220-11230.	13.7	53
100	Loading quantum dots into thermo-responsive microgels by reversible transfer from organic solvents to water. Journal of Materials Chemistry, 2008, 18, 763.	6.7	52
101	Formation of Lenticular Platelet Micelles via the Interplay of Crystallization and Chain Stretching: Solution Self-Assembly of Poly(ferrocenyldimethylsilane)- <i>block</i> -poly(2-vinylpyridine) with a Crystallizable Core-Forming Metalloblock. Macromolecules, 2012, 45, 3883-3891.	4.8	52
102	Metal-Chelating Polymers by Anionic Ring-Opening Polymerization and Their Use in Quantitative Mass Cytometry. Biomacromolecules, 2012, 13, 2359-2369.	5.4	51
103	Competitive Self-Assembly Kinetics as a Route To Control the Morphology of Core-Crystalline Cylindrical Micelles. Journal of the American Chemical Society, 2018, 140, 2619-2628.	13.7	51
104	INTRAMOLECULAR EXCIMER FLUORESCENCE: A NEW PROBE OF PHASE TRANSITIONS IN SYNTHETIC PHOSPHOLIPID MEMBRANES. Photochemistry and Photobiology, 1980, 31, 539-545.	2.5	50
105	Characterization of pyrene end-labeled poly(ethylene glycol) by high resolution MALDI time-of-flight mass spectrometry. Macromolecular Rapid Communications, 1996, 17, 59-64.	3.9	47
106	Polypyrrole nanoparticles as a thermal transducer of NIR radiation in hot-melt adhesives. Journal of Materials Chemistry, 2007, 17, 4309.	6.7	47
107	Investigating the influence of block copolymer micelle length on cellular uptake and penetration in a multicellular tumor spheroid model. Nanoscale, 2021, 13, 280-291.	5.6	47
108	The Interaction of Sodium Dodecylsulfate with (Hydroxypropyl)Cellulose. Polymer Journal, 1990, 22, 482-488.	2.7	46

#	Article	IF	CITATIONS
109	Curious Results with Palladium- and Platinum-Carrying Polymers in Mass Cytometry Bioassays and an Unexpected Application as a Dead Cell Stain. Biomacromolecules, 2011, 12, 3997-4010.	5.4	46
110	Formation and crosslinking of latex films through the reaction of acetoacetoxy groups with diamines under ambient conditions. Journal of Coatings Technology, 1998, 70, 57-68.	0.7	45
111	Improving Lanthanide Nanocrystal Colloidal Stability in Competitive Aqueous Buffer Solutions using Multivalent PEG-Phosphonate Ligands. Langmuir, 2012, 28, 12861-12870.	3.5	44
112	A microphase model for sterically stabilized polymer colloids: Fluorescence energy transfer from naphthalene-labeled dispersions. Journal of Polymer Science, Polymer Letters Edition, 1983, 21, 1011-1018.	0.4	43
113	Metal-containing polystyrene beads as standards for mass cytometry. Journal of Analytical Atomic Spectrometry, 2010, 25, 260.	3.0	43
114	Microfibres and macroscopic films from the coordination-driven hierarchical self-assembly of cylindrical micelles. Nature Communications, 2016, 7, 12371.	12.8	43
115	Film Formation and Polymer Diffusion in Poly(vinyl acetate-co-butyl acrylate) Latex Films. Temperature Dependence. Macromolecules, 2003, 36, 5804-5814.	4.8	42
116	Effect of Hard Polymer Filler Particles on Polymer Diffusion in a Low-TgLatex Film. Macromolecules, 1998, 31, 5290-5299.	4.8	41
117	Solution characterization of the novel organometallic polymer poly(ferrocenyldimethylsilane). Journal of Polymer Science, Part B: Polymer Physics, 2000, 38, 3032-3041.	2.1	41
118	Polymer Diffusion in PBMA Latex Films Using a Polymerizable Benzophenone Derivative as an Energy Transfer Acceptor. Macromolecules, 2003, 36, 8749-8760.	4.8	40
119	Pulsed Field Gradient NMR Studies of Polymer Adsorption on Colloidal CdSe Quantum Dots. Journal of Physical Chemistry B, 2008, 112, 1626-1633.	2.6	40
120	Interdiffusion vs Cross-Linking Rates in Isobutoxyacrylamide-Containing Latex Coatings. Macromolecules, 2001, 34, 7306-7314.	4.8	39
121	Synthesis and Solution Self-Assembly of Coilâ^'Crystallineâ^'Coil Polyferrocenylphosphine-b-polyferrocenylsilane-b-polysiloxane Triblock Copolymers. Macromolecules, 2002, 35, 9146-9150.	4.8	39
122	Modular Synthesis of Polyferrocenylsilane Block Copolymers by Cu-Catalyzed Alkyne/Azide "Click― Reactions. Macromolecules, 2013, 46, 1296-1304.	4.8	39
123	Quantification of Surface Ligands on NaYF4 Nanoparticles by Three Independent Analytical Techniques. Chemistry of Materials, 2015, 27, 4899-4910.	6.7	39
124	Synthesis of Uniform NaLnF <sub>4</sub> (Ln: Sm to Ho) Nanoparticles for Mass Cytometry. Journal of Physical Chemistry C, 2016, 120, 6269-6280.	3.1	39
125	Panitumumab Modified with Metal-Chelating Polymers (MCP) Complexed to <sup>111</sup> In and <sup>177</sup> Lu—An EGFR-Targeted Theranostic for Pancreatic Cancer. Molecular Pharmaceutics, 2018, 15, 1150-1159.	4.6	39
126	Explosive dissolution and trapping of block copolymer seed crystallites. Nature Communications, 2018, 9, 1158.	12.8	39

#	Article	IF	CITATIONS
127	Synthesis and self-assembly of dendritic-helical block copolypeptides. Soft Matter, 2006, 2, 957.	2.7	38
128	Templated Fabrication of Fiber-Basket Polymersomes via Crystallization-Driven Block Copolymer Self-Assembly. Journal of the American Chemical Society, 2014, 136, 16676-16682.	13.7	38
129	Synthesis of PMMA Microparticles with a Narrow Size Distribution by Photoinitiated RAFT Dispersion Polymerization with a Macromonomer as the Stabilizer. Macromolecules, 2014, 47, 6856-6866.	4.8	38
130	Transformation and patterning of supermicelles using dynamic holographic assembly. Nature Communications, 2015, 6, 10009.	12.8	38
131	Rodlike Block Copolymer Micelles of Controlled Length in Water Designed for Biomedical Applications. Macromolecules, 2019, 52, 5231-5244.	4.8	38
132	Synergistic self-seeding in one-dimension: a route to patchy and block comicelles with uniform and controllable length. Chemical Science, 2019, 10, 2280-2284.	7.4	38
133	Influence of a coalescing aid on polymer diffusion in poly(butyl methacrylate) latex films. Die Makromolekulare Chemie Rapid Communications, 1993, 14, 345-349.	1.1	37
134	Uniform 1D Micelles and Patchy & Block Comicelles via Scalable, One-Step Crystallization-Driven Block Copolymer Self-Assembly. Journal of the American Chemical Society, 2021, 143, 6266-6280.	13.7	37
135	Copolymerization kinetics of 4-methoxystyrene with methyl methacrylate and 4-methoxystyrene with styrene: A test of the penultimate model. Journal of Polymer Science Part A, 1990, 28, 2097-2106.	2.3	36
136	Cross-Linking, Miscibility, and Interface Structure in Blends of Poly(2-ethylhexyl methacrylate) Copolymers. An Energy Transfer Study. Macromolecules, 2000, 33, 5850-5862.	4.8	36
137	Solvent penetration and photoresist dissolution: A fluorescence quenching and interferometry study. Journal of Applied Polymer Science, 1988, 35, 2099-2116.	2.6	35
138	Kinetics of Fusion and Fragmentation Nonionic Micelles:Â Triton X-100. Langmuir, 1999, 15, 4697-4700.	3.5	35
139	Effect of Gel Content on Polymer Diffusion in Poly(vinyl acetate-co-dibutyl maleate) Latex Films. Macromolecules, 2004, 37, 4247-4253.	4.8	35
140	Fiberâ€Like Micelles from the Crystallizationâ€Driven Selfâ€Assembly of Poly(3â€heptylselenophene)â€ <i>block</i> â€Polystyrene. Macromolecular Chemistry and Physics, 2015, 216, 685-695.	2.2	35
141	MicroPET/CT imaging of patient-derived pancreatic cancer xenografts implanted subcutaneously or orthotopically in NOD-scid mice using 64Cu-NOTA-panitumumab F(ab')2 fragments. Nuclear Medicine and Biology, 2015, 42, 71-77.	0.6	35
142	Dye distribution in fluorescent-labeled latex prepared by emulsion polymerization. Journal of Polymer Science Part A, 1994, 32, 1497-1505.	2.3	34
143	Phosphorescent Oxygen Sensors Utilizing Sulfurâ~'Nitrogenâ~'Phosphorus Polymer Matrixes:Â Synthesis, Characterization, and Evaluation of Poly(thionylphosphazene)-b-Poly(tetrahydrofuran) Block Copolymers. Analytical Chemistry, 2000, 72, 1894-1904.	6.5	34
144	Surface Functionalization Methods To Enhance Bioconjugation in Metal-Labeled Polystyrene Particles. Macromolecules, 2011, 44, 4801-4813.	4.8	34

#	Article	IF	CITATIONS
145	Synthesis of Polyglutamide-Based Metal-Chelating Polymers and Their Site-Specific Conjugation to Trastuzumab for Auger Electron Radioimmunotherapy. Biomacromolecules, 2014, 15, 2027-2037.	5.4	34
146	Lanthanide nanoparticles for high sensitivity multiparameter single cell analysis. Chemical Science, 2019, 10, 2965-2974.	7.4	34
147	Oxygen Diffusion and Permeability in Alkylaminothionylphosphazene Films Intended for Phosphorescence Barometry Applications. Macromolecules, 2000, 33, 5693-5701.	4.8	33
148	Effect of Silica as Fillers on Polymer Interdiffusion in Poly(butyl methacrylate) Latex Films. Macromolecules, 2002, 35, 7387-7399.	4.8	33
149	Emulsion copolymerization of vinyl acetate and butyl acrylate in the presence of fluorescent dyes. Journal of Polymer Science Part A, 2002, 40, 1594-1607.	2.3	33
150	Functional PEG–PAMAM-Tetraphosphonate Capped NaLnF <sub>4</sub> Nanoparticles and their Colloidal Stability in Phosphate Buffer. Langmuir, 2014, 30, 6980-6989.	3.5	33
151	PMMA Microspheres with Embedded Lanthanide Nanoparticles by Photoinitiated Dispersion Polymerization with a Carboxy-Functional Macro-RAFT Agent. Macromolecules, 2015, 48, 3629-3640.	4.8	33
152	Toward Uniform Nanofibers with a π-Conjugated Core: Optimizing the "Living―Crystallization-Driven Self-Assembly of Diblock Copolymers with a Poly(3-octylthiophene) Core-Forming Block. Macromolecules, 2018, 51, 5101-5113.	4.8	33
153	Synthesis of the First Organometallic Miktoarm Star Polymer. Macromolecular Rapid Communications, 2003, 24, 403-407.	3.9	32
154	Effect of Polymer Composition on Polymer Diffusion in Poly(butyl acrylate- <i>co</i> -methyl) Tj ETQq0 0 0 rgBT /	Overlock : 4.8	10 Tf 50 382 1 32
155	Crystallization-Driven Solution Self-Assembly of μ-ABC Miktoarm Star Terpolymers with Core-Forming Polyferrocenylsilane Blocks. Macromolecules, 2014, 47, 8420-8428.	4.8	32
156	Synthesis and crystallization-driven solution self-assembly of polyferrocenylsilane diblock copolymers with polymethacrylate corona-forming blocks. Polymer Chemistry, 2014, 5, 1923-1929.	3.9	32
157	Stability and Biodistribution of Thiol-Functionalized and <sup>177</sup> Lu-Labeled Metal Chelating Polymers Bound to Gold Nanoparticles. Biomacromolecules, 2016, 17, 1292-1302.	5.4	32
158	Pulsed laser study of the propagation kinetics of tert-butyl methacrylate. Die Makromolekulare Chemie Rapid Communications, 1993, 14, 213-215.	1.1	31
159	Supramolecular Organometallic Polymer Chemistry: Self-Assembly of a Novel Poly(ferrocene)-b-polysiloxane-b-poly(ferrocene) Triblock Copolymer in Solution. Angewandte Chemie - International Edition, 1999, 38, 2570-2573.	13.8	31
160	Fiberlike Micelles Formed by Living Epitaxial Growth from Blends of Polyferrocenylsilane Block Copolymers. Macromolecular Rapid Communications, 2010, 31, 934-938.	3.9	31
161	Synthesis, self-assembly and photophysical properties of oligo(2,5-dihexyloxy-1,4-phenylene) Tj ETQq1 1 0.7843	14 rgBT /C 2:7	Overlock 10 Tf
162	Functionalization of Cellulose Nanocrystals with PEG-Metal-Chelating Block Copolymers via	3.5	31

Controlled Conjugation in Aqueous Media. ACS Omega, 2016, 1, 93-107.

#	Article	IF	CITATIONS
163	Effect of Hydroplasticization on Polymer Diffusion in Poly(butyl acrylate- <i>co</i> -methyl) Tj ETQq1 1 0.784314 r Macromolecules, 2010, 43, 975-985.	gBT /Over 4.8	lock 10 Tf 5 30
164	Polyferrocenylsilane Crystals in Nanoconfinement: Fragmentation, Dissolution, and Regrowth of Cylindrical Block Copolymer Micelles with a Crystalline Core. Macromolecules, 2012, 45, 8363-8372.	4.8	30
165	Hierarchical Polymer–Carbon Nanotube Hybrid Mesostructures by Crystallization-Driven Self-Assembly. ACS Nano, 2015, 9, 10673-10685.	14.6	30
166	THE DYNAMICS OF POLYMER CYCLIZATION 3. EXCLUDED VOLUME EFFECTS IN THE END-TO-END CYCLIZATION OF POLYSTYRENE PROBED BY INTRAMOLECULAR PYRENE EXCIMER FORMATION. Annals of the New York Academy of Sciences, 1981, 366, 75-92.	3.8	29
167	Synthesis of Meth(acrylate) Diblock Copolymers Bearing a Fluorescent Dye at the Junction Using A Hydroxyl-Protected Initiator and the Combination of Anionic Polymerization and Controlled Radical Polymerization. Macromolecules, 2001, 34, 696-705.	4.8	29
168	Interface Thickness of a Styreneâ^'Methyl Methacrylate Block Copolymer in the Lamella Phase by Direct Nonradiative Energy Transfer. Macromolecules, 2001, 34, 5238-5248.	4.8	29
169	Synthesis, characterization, and emulsion polymerization of polymerizable coumarin derivatives. Journal of Polymer Science Part A, 2004, 42, 3479-3489.	2.3	29
170	Synthesis of chromophore-labelled polystyrene/poly(ethylene oxide) diblock copolymers. Die Makromolekulare Chemie, 1993, 194, 1411-1420.	1.1	28
171	Copolymer microgels by precipitation polymerisation of N-vinylcaprolactam and N-isopropylacrylamides in aqueous medium. Colloid and Polymer Science, 2013, 291, 21-31.	2.1	28
172	Conductive, Monodisperse Polyaniline Nanofibers of Controlled Length Using Wellâ€Đefined Cylindrical Block Copolymer Micelles as Templates. Chemistry - A European Journal, 2013, 19, 13030-13039.	3.3	28
173	Metal-Chelating Polymers (MCPs) with Zwitterionic Pendant Groups Complexed to Trastuzumab Exhibit Decreased Liver Accumulation Compared to Polyanionic MCP Immunoconjugates. Biomacromolecules, 2015, 16, 3613-3623.	5.4	28
174	PFS- <i>b</i> -PNIPAM: A First Step toward Polymeric Nanofibrillar Hydrogels Based on Uniform Fiber-Like Micelles. Macromolecules, 2016, 49, 4265-4276.	4.8	28
175	Block copolymer self-assembly: Polydisperse corona-forming blocks leading to uniform morphologies. CheM, 2021, 7, 2800-2821.	11.7	28
176	The influence of PEG macromonomers on the size and properties of thermosensitive aqueous microgels. Colloid and Polymer Science, 2009, 287, 269-275.	2.1	27
177	Smart Polymer Nanoparticles Designed for Environmentally Compliant Coatings. Journal of the American Chemical Society, 2011, 133, 11299-11307.	13.7	27
178	Liquid Crystalline Phase Behavior of Well-Defined Cylindrical Block Copolymer Micelles Using Synchrotron Small-Angle X-ray Scattering. Macromolecules, 2015, 48, 1579-1591.	4.8	27
179	Liposome-Encapsulated NaLnF <sub>4</sub> Nanoparticles for Mass Cytometry: Evaluating Nonspecific Binding to Cells. Chemistry of Materials, 2017, 29, 4980-4990.	6.7	27
180	Cylindrical Micelles with "Patchy―Coronas from the Crystallization-Driven Self-Assembly of ABC Triblock Terpolymers with a Crystallizable Central Polyferrocenyldimethylsilane Segment. Macromolecules, 2018, 51, 222-231.	4.8	27

#	Article	IF	CITATIONS
181	Polymer Interdiffusion vs Cross-Linking in Carboxylic Acidâ^ Carbodiimide Latex Films. Effect of Annealing Temperature, Reactive Group Concentration, and Carbodiimide Substituent. Macromolecules, 2006, 39, 1425-1435.	4.8	26
182	The onset of polymer diffusion in a drying acrylate latex: how water initially retards coalescence but ultimately enhances diffusion. Journal of Coatings Technology Research, 2008, 5, 157-168.	2.5	26
183	Trastuzumab Labeled to High Specific Activity with <sup>111</sup> In by Site-Specific Conjugation to a Metal-Chelating Polymer Exhibits Amplified Auger Electron-Mediated Cytotoxicity on HER2-Positive Breast Cancer Cells. Molecular Pharmaceutics, 2015, 12, 1951-1960.	4.6	26
184	Lateral Growth of 1D Core-Crystalline Micelles upon Annealing in Solution. Macromolecules, 2016, 49, 7004-7014.	4.8	26
185	Solvent effects leading to a variety of different 2D structures in the self-assembly of a crystalline-coil block copolymer with an amphiphilic corona-forming block. Chemical Science, 2020, 11, 4631-4643.	7.4	26
186	Effect of Pendant Group Structure on the Hydrolytic Stability of Polyaspartamide Polymers under Physiological Conditions. Biomacromolecules, 2012, 13, 1296-1306.	5.4	25
187	Fluorescence techniques in the study of polymer colloids. Polymer Engineering and Science, 1984, 24, 87-97.	3.1	24
188	Non-ionic surfactant effects on polymer diffusion in poly(butyl methacrylate) latex films. Macromolecular Rapid Communications, 1995, 16, 861-868.	3.9	24
189	Bio-functional, lanthanide-labeled polymer particles by seeded emulsion polymerization and their characterization by novel ICP-MS detection. Journal of Analytical Atomic Spectrometry, 2010, 25, 269-281.	3.0	24
190	How a Small Change of Oligo( <i>p</i> -phenylenevinylene) Chain Length Affects Self-Seeding of Oligo( <i>p</i> -phenylenevinylene)-Containing Block Copolymers. Macromolecules, 2020, 53, 1831-1841.	4.8	24
191	Title is missing!. Die Makromolekulare Chemie, 1992, 193, 1987-1994.	1.1	23
192	Morphology evolution and location of ethylene-propylene copolymer in annealed polyethylene/polypropylene blends. Journal of Polymer Science, Part B: Polymer Physics, 1997, 35, 979-991.	2.1	23
193	Epoxy-functionalized, low glass-transition temperature latex. I. Synthesis, characterizations, and polymer interdiffusion. Journal of Polymer Science Part A, 2002, 40, 2609-2625.	2.3	23
194	Organometallic–Polypeptide Diblock Copolymers: Synthesis by Diels–Alder Coupling and Crystallization-Driven Self-Assembly to Uniform Truncated Elliptical Lamellae. Macromolecules, 2014, 47, 2604-2615.	4.8	23
195	Polymer diffusion in latex films at ambient temperature. Journal of Polymer Science, Part B: Polymer Physics, 1998, 36, 1129-1139.	2.1	22
196	Polymerizable benzophenone derivatives for labeling vinyl acetate-butylacrylate latex particles. Journal of Polymer Science Part A, 2002, 40, 3001-3011.	2.3	22
197	Synthesis, Characterization, and AFM Studies of Dendronized Polyferrocenylsilanes. Macromolecules, 2006, 39, 7922-7930.	4.8	22
198	The synthesis and characterization of lanthanide-encoded poly(styrene-co-methacrylic acid) microspheres. Polymer, 2011, 52, 5040-5052.	3.8	22

#	Article	IF	CITATIONS
199	A High-Sensitivity Lanthanide Nanoparticle Reporter for Mass Cytometry: Tests on Microgels as a Proxy for Cells. Langmuir, 2014, 30, 3142-3153.	3.5	22
200	A Critical Evaluation of Direct Energy Transfer as a Tool for Analysis of Nanoscale Morphologies in Polymers. Application to Block Copolymer Interfaces. Journal of Physical Chemistry B, 1998, 102, 7960-7970.	2.6	21
201	Pyrene Excimer Kinetics in Micellelike Aggregates in a C20-HASE Associating Polymerâ€. Langmuir, 2000, 16, 8664-8671.	3.5	21
202	Temperature Dependence of Polymer Diffusion in Poly(vinyl acetate-co-dibutyl maleate) Latex Films. Macromolecules, 2004, 37, 2299-2306.	4.8	21
203	Synthesis of Branched Poly(butyl methacrylate) via Semicontinuous Emulsion Polymerization. Macromolecules, 2008, 41, 4220-4225.	4.8	21
204	Dual-Purpose Polymer Labels for Fluorescent and Mass Cytometric Affinity Bioassays. Biomacromolecules, 2013, 14, 1503-1513.	5.4	21
205	Manipulation and Deposition of Complex, Functional Block Copolymer Nanostructures Using Optical Tweezers. ACS Nano, 2019, 13, 3858-3866.	14.6	21
206	Effect of Soft Filler Particles on Polymer Diffusion in Poly(butyl methacrylate) Latex Films. Macromolecules, 2001, 34, 6039-6051.	4.8	20
207	Photocleavage of the Corona Chains of Rigid-Rod Block Copolymer Micelles. Macromolecules, 2015, 48, 2254-2262.	4.8	20
208	Water-Dispersible, Colloidally Stable, Surface-Functionalizable Uniform Fiberlike Micelles Containing a π-Conjugated Oligo( <i>p</i> -phenylenevinylene) Core of Controlled Length. Macromolecules, 2020, 53, 8009-8019.	4.8	20
209	Title is missing!. Die Makromolekulare Chemie, 1987, 188, 2621-2629.	1.1	19
210	Interface characterization in latex blend films by fluorescence energy transfer. Journal of Polymer Science, Part B: Polymer Physics, 1998, 36, 1115-1128.	2.1	19
211	Epoxy-functionalized, low-glass-transition-temperature latex. II. Interdiffusion versus crosslinking in the presence of a diamine. Journal of Polymer Science Part A, 2002, 40, 4098-4116.	2.3	19
212	Compatibility of Chlorinated Polyolefin with the Components of Thermoplastic Polyolefin:Â A Study by Laser Scanning Confocal Fluorescence Microscopy. Macromolecules, 2004, 37, 6544-6552.	4.8	19
213	Polymer Diffusion in Gel-Containing Poly(vinyl acetate-co-dibutyl maleate) Latex Films. Macromolecules, 2005, 38, 4393-4402.	4.8	19
214	Intracellular Routing in Breast Cancer Cells of Streptavidin-Conjugated Trastuzumab Fab Fragments Linked to Biotinylated Doxorubicin-Functionalized Metal Chelating Polymers. Biomacromolecules, 2014, 15, 715-725.	5.4	19
215	Tantalum Oxide Nanoparticle-Based Mass Tag for Mass Cytometry. Analytical Chemistry, 2020, 92, 5741-5749.	6.5	19
216	Influence of Entanglements on the Time Dependence of Mixing in Nonradiative Energy Transfer Studies of Polymer Diffusion in Latex Films. Macromolecules, 2001, 34, 6029-6038.	4.8	18

#	Article	IF	CITATIONS
217	Seeded Growth and Solventâ€Induced Fragmentation of Fiberlike Polyferrocenylsilane–Polyisoprene Block Copolymer Micelles. Macromolecular Rapid Communications, 2010, 31, 928-933.	3.9	18
218	Hybrid nanogels by encapsulation of lanthanide-doped LaF3 nanoparticles as elemental tags for detection by atomic mass spectrometry. Journal of Materials Chemistry, 2010, 20, 5141.	6.7	18
219	Evaluation of the Cross Section of Elongated Micelles by Static and Dynamic Light Scattering. Journal of Physical Chemistry B, 2012, 116, 4328-4337.	2.6	18
220	Fluorous Cylindrical Micelles of Controlled Length by Crystallization-Driven Self-Assembly of Block Copolymers in Fluorinated Media. ACS Macro Letters, 2015, 4, 187-191.	4.8	18
221	Self-Seeding of Oligo( <i>p</i> -phenylenevinylene)- <i>b</i> -poly(2-vinylpyridine) Micelles: Effect of Metal Ions. Macromolecules, 2021, 54, 6705-6717.	4.8	18
222	Synthesis and Microstructure Characterization of Dye-Labeled Poly(vinyl acetate-co-dibutyl maleate) Latex for Energy Transfer Experiments. Macromolecules, 2003, 36, 8139-8147.	4.8	17
223	Effect of molecular weight distribution on polymer diffusion during film formation of two-component high-/low-molecular weight latex particles. Polymer, 2012, 53, 2652-2663.	3.8	17
224	How a Small Modification of the Corona-Forming Block Redirects the Self-Assembly of Crystalline–Coil Block Copolymers in Solution. Macromolecules, 2016, 49, 7975-7984.	4.8	17
225	Effect of Concentration on the Dissolution of One-Dimensional Polymer Crystals: A TEM and NMR Study. Macromolecules, 2019, 52, 208-216.	4.8	17
226	Metal-Encoded Polystyrene Microbeads as a Mass Cytometry Calibration/Normalization Standard Covering Channels from Yttrium (89 amu) to Bismuth (209 amu). Analytical Chemistry, 2020, 92, 999-1006.	6.5	17
227	Crystallization-Driven Self-Assembly of a Block Copolymer with Amphiphilic Pendant Groups. Macromolecules, 2021, 54, 930-940.	4.8	17
228	An Enzymeâ€Like Activity Nanoprobe Based on Fe(III)–Rutin Hydrate Biomineral for MR Imaging and Therapy of Triple Negative Breast Cancer. Advanced Functional Materials, 2022, 32, .	14.9	17
229	Polymerizable anthracene derivatives for labeling emulsion copolymers. Journal of Polymer Science Part A, 2001, 39, 1495-1504.	2.3	16
230	Polymer diffusion in high-M/low-M hard-soft latex blends. Colloid and Polymer Science, 2009, 287, 367-378.	2.1	16
231	The Effect of Metal-Chelating Polymers (MCPs) for 111In Complexed via the Streptavidin-Biotin System to Trastuzumab Fab Fragments on Tumor and Normal Tissue Distribution in Mice. Pharmaceutical Research, 2013, 30, 104-116.	3.5	16
232	Radioimmunotherapy of PANC-1 Human Pancreatic Cancer Xenografts in NRG Mice with Panitumumab Modified with Metal-Chelating Polymers Complexed to <sup>177</sup> Lu. Molecular Pharmaceutics, 2019, 16, 768-778.	4.6	16
233	A comparison of DFO and DFO* conjugated to trastuzumab-DM1 for complexing 89Zr – In vitro stability and in vivo microPET/CT imaging studies in NOD/SCID mice with HER2-positive SK-OV-3 human ovarian cancer xenografts. Nuclear Medicine and Biology, 2020, 84-85, 11-19.	0.6	16
234	Novel Morphology Evolution in Thick Films of a Polymer Blend. Macromolecules, 2002, 35, 3321-3324.	4.8	15

#	Article	IF	CITATIONS
235	Interface Orientation and Chain Conformation in Simulated Symmetric Diblock Copolymer Lamellar Systems. Macromolecular Theory and Simulations, 2005, 14, 9-20.	1.4	15
236	Preparation and photo/chemical-activation of wormlike network micelles of core–shell quantum dots and block copolymer hybrids. Journal of Materials Chemistry, 2011, 21, 9692.	6.7	15
237	Biotinylated Polyacrylamide-Based Metal-Chelating Polymers and Their Influence on Antigen Recognition Following Conjugation to a Trastuzumab Fab Fragment. Biomacromolecules, 2012, 13, 2831-2842.	5.4	15
238	Influence of Lu <sup>3+</sup> Doping on the Crystal Structure of Uniform Small (5 and 13 nm) NaLnF <sub>4</sub> Upconverting Nanocrystals. Journal of Physical Chemistry C, 2017, 121, 18178-18185.	3.1	15
239	Characterization of an Aqueous Dispersion of a Hydrophilic Polyisocyanate for Waterborne Two-Pack Polyurethane Coatings. ACS Applied Polymer Materials, 2020, 2, 1491-1499.	4.4	15
240	Spherulite‣ike Micelles. Angewandte Chemie - International Edition, 2021, 60, 10950-10956.	13.8	15
241	Cyclization dynamics of polymers, 26. End-to-end cyclization of polystyrene in mixed solvents. Effect of chain length. Die Makromolekulare Chemie, 1989, 15, 113-125.	1.1	14
242	Thermal decomposition of amide and imide derivatives of maleated polyethylene. Journal of Polymer Science Part A, 2000, 38, 730-740.	2.3	14
243	Morphology of Poly(2-ethylhexyl methacrylate):Poly(butyl methacrylate) Latex Blend Films. Macromolecules, 2001, 34, 2298-2314.	4.8	14
244	Characterizing the Quenching Process for Phosphorescent Dyes in Poly[((n-butylamino)thionyl)phosphazene] Films. Journal of Physical Chemistry B, 2003, 107, 13349-13356.	2.6	14
245	Understanding particle formation in surfactant-free waterborne coatings prepared by emulsification of pre-formed polymers. Polymer Chemistry, 2017, 8, 2931-2941.	3.9	14
246	Creating Biomorphic Barbed and Branched Mesostructures in Solution through Block Copolymer Crystallization. Angewandte Chemie - International Edition, 2018, 57, 17205-17210.	13.8	14
247	Functionalization of Cellulose Nanocrystals with POEGMA Copolymers via Copper-Catalyzed Azide–Alkyne Cycloaddition for Potential Drug-Delivery Applications. Biomacromolecules, 2020, 21, 2014-2023.	5.4	14
248	Dual-Receptor-Targeted (DRT) Radiation Nanomedicine Labeled with <sup>177</sup> Lu Is More Potent for Killing Human Breast Cancer Cells That Coexpress HER2 and EGFR Than Single-Receptor-Targeted (SRT) Radiation Nanomedicines. Molecular Pharmaceutics, 2020, 17, 1226-1236.	4.6	14
249	Diffusion reaction in restricted spaces of spherical symmetry: Surface quenching of luminescence. Journal of Chemical Physics, 1992, 97, 1554-1561.	3.0	13
250	Synthesis, characterization, and stability of carbodiimide groups in carbodiimide-functionalized latex dispersions and films. Journal of Polymer Science Part A, 2000, 38, 855-869.	2.3	13
251	Monodisperse, micrometer-sized low molar mass polystyrene particles by two-stage dispersion polymerization. Polymer, 2006, 47, 4557-4563.	3.8	13
252	Systematic study of the fluorescence decays of aminoâ€coumarin dyes in polymer matrices. Journal of Polymer Science, Part B: Polymer Physics, 2007, 45, 2333-2343.	2.1	13

#	Article	IF	CITATIONS
253	Synthesis and characterization of a naphthalimide–dye end-labeled copolymer by reversible addition–fragmentation chain transfer (RAFT) polymerization. Canadian Journal of Chemistry, 2011, 89, 317-325.	1.1	13
254	Continuous and Segmented Semiconducting Fiberâ€like Nanostructures with Spatially Selective Functionalization by Living Crystallizationâ€Driven Selfâ€Assembly. Angewandte Chemie, 2020, 132, 8309-8316.	2.0	13
255	An â€~â€~on''â€gated photomultiplier circuit for the determination of phosphorescence lifetimes. Review Scientific Instruments, 1990, 61, 3726-3728.	of 1.3	12
256	Title is missing!. Journal of Inorganic and Organometallic Polymers, 1998, 8, 215-224.	1.5	12
257	Effect of Hyperbranched Poly(butyl methacrylate) on Polymer Diffusion in Poly(butyl) Tj ETQq1 1 0.784314 rgBT	/Oyerlock 4.8	19Jf 50 582
258	Monodisperse Cylindrical Micelles of Controlled Length with a Liquidâ€Crystalline Perfluorinated Core by 1D "Self‧eeding― Angewandte Chemie, 2016, 128, 11564-11568.	2.0	12
259	Monitoring Collapse of Uniform Cylindrical Brushes with a Thermoresponsive Corona in Water. ACS Macro Letters, 2018, 7, 166-171.	4.8	12
260	Influence of Cubic-to-Hexagonal-Phase Transformation on the Uniformity of NaLnF <sub>4</sub> (Ho,) Tj ETQq0 (	0 0 rgBT /0	Overlock 10 <sup>-</sup>
261	Enabling Indium Channels for Mass Cytometry by Using Reinforced Cyclam-Based Chelating Polylysine. Bioconjugate Chemistry, 2020, 31, 2103-2115.	3.6	12
262	An Amphiphilic Corona-Forming Block Promotes Formation of a Variety of 2D Platelets via Crystallization-Driven Block Copolymer Self-Assembly. Macromolecules, 2021, 54, 9761-9772.	4.8	12
263	Substituent effect and rearrangements in the electron-impact spectra of long chain esters ofm-andp-methoxybenzoic acid. Organic Mass Spectrometry, 1975, 10, 339-346.	1.3	11
264	Synthesis and Solution Selfâ€Assembly of Polyisopreneâ€ <i>block</i> â€poly(ferrocenylmethylsilane): A Diblock Copolymer with an Atactic but Semicrystalline Coreâ€Forming Metalloblock. Macromolecular Chemistry and Physics, 2016, 217, 1671-1682.	2.2	11
265	Monte Carlo simulation of radiation transport and dose deposition from locally released gold nanoparticles labeled with <sup>111</sup> In, <sup>177</sup> Lu or <sup>90</sup> Y incorporated into tissue implantable depots. Physics in Medicine and Biology, 2017, 62, 8581-8599.	3.0	11
266	NMR Study of the Dissolution of Core-Crystalline Micelles. Macromolecules, 2018, 51, 3279-3289.	4.8	11
267	Mechanistic study of the formation of fiber-like micelles with a π-conjugated oligo(p-phenylenevinylene) core. Journal of Colloid and Interface Science, 2020, 560, 50-58.	9.4	11
268	Crystallization-Driven Self-Assembly of Amphiphilic Triblock Terpolymers With Two Corona-Forming Blocks of Distinct Hydrophilicities. Macromolecules, 2020, 53, 6576-6588.	4.8	11
269	Understanding the Dissolution and Regrowth of Core-Crystalline Block Copolymer Micelles: A Scaling Approach. Macromolecules, 2020, 53, 10198-10211.	4.8	11

	Probing the Analogy between Living Crystallization-Driven Self-Assembly and Living Covalent		
270	Polymerizations: Length-Independent Growth Behavior for 1D Block Copolymer Nanofibers.	4.8	11
	Macromolecules, 2022, 55, 359-369.		

#	Article	IF	CITATIONS
271	Polymeric dipicolylamine based mass tags for mass cytometry. Chemical Science, 2022, 13, 3233-3243.	7.4	11
272	Transient effects in diffusion-controlled polymer cyclization. Die Makromolekulare Chemie, 1989, 190, 1333-1343.	1.1	10
273	Investigation of morphology and miscibility of isotactic polypropylene, ethyleneâ€butene copolymer and chlorinated polyolefin blends via LSCFM, SEM, WAXD, and DMA. Polymers for Advanced Technologies, 2009, 20, 235-245.	3.2	10
274	Synthesis and solution self-assembly of block copolymers with a gradient, crystallizable polyferrocenylsilane core-forming metalloblock. Soft Matter, 2013, 9, 8569.	2.7	10
275	Differential Binding Models for Direct and Reverse Isothermal Titration Calorimetry. Journal of Physical Chemistry B, 2016, 120, 2077-2086.	2.6	10
276	A metal-chelating polymer for chelating zirconium and its use in mass cytometry. European Polymer Journal, 2019, 120, 109175.	5.4	10
277	Radioimmunotherapy of PANC-1 human pancreatic cancer xenografts in NOD/SCID or NRG mice with Panitumumab labeled with Auger electron emitting, 111In or β-particle emitting, 177Lu. EJNMMI Radiopharmacy and Chemistry, 2020, 5, 22.	3.9	10
278	Hydrocarbon dispersions of acrylic microspheres with polar surface functionality. Journal of Polymer Science Part A, 1994, 32, 2333-2344.	2.3	9
279	Characterization of the ground state pyrene complex in ethylene-propylene copolymer solutions. Journal of Polymer Science, Part B: Polymer Physics, 1995, 33, 1173-1181.	2.1	9
280	Effect of oligomers on the polymer diffusion rate in poly(butyl methacrylate) latex films. Journal of Polymer Science Part A, 2000, 38, 3933-3943.	2.3	9
281	Effect of a Water-Soluble Polymer on Polymer Interdiffusion in P(MMA-co-BA) Latex Films. Macromolecular Chemistry and Physics, 2003, 204, 1933-1940.	2.2	9
282	Poly(vinyl acetate-co-dibutyl maleate) latex films in the presence of grafted and post-added poly(vinyl) Tj ETQqO	0 0 rgBT / 2.9	Overlock 10 T
283	The release and extraction of lanthanide ions from metal-encoded poly (styrene-co-methacrylic acid) microspheres. Polymer, 2012, 53, 998-1004.	3.8	9
284	Temperature-Invariant Aqueous Microgels as Hosts for Biomacromolecules. Biomacromolecules, 2015, 16, 3134-3144.	5.4	9
285	Cvclization of polystyrene chains in the crossover region between theta and good solvents: Cyclization dynamics of polymers 12. Journal of Polymer Science, Polymer Symposia, 1985, 73, 113-120.	0.1	8
286	Application of fluorescence quenching techniques to the study of emulsion polymerization and latex characterization. Makromolekulare Chemie Macromolecular Symposia, 1993, 70-71, 107-117.	0.6	8
287	Visualizing Nanoscale Coronal Segregation in Rod‣ike Micelles Formed by Coâ€Assembly of Binary Block Copolymer Blends. Macromolecular Rapid Communications, 2018, 39, e1800397.	3.9	8
288	Molecular Aspects of Film Formation of Partially Cross-Linked Water-Borne Secondary Dispersions that Show Skin Formation upon Drying. Macromolecules, 2019, 52, 9536-9544.	4.8	8

#	Article	IF	CITATIONS
289	Single-step self-assembly to uniform fiber-like core-crystalline block copolymer micelles. Chemical Communications, 2020, 56, 4595-4598.	4.1	8
290	The role of cooling rate in crystallization-driven block copolymer self-assembly. Chemical Science, 2022, 13, 396-409.	7.4	8
291	Fluorescence Studies of Polymer Association in Water. Advances in Chemistry Series, 1993, , 485-505.	0.6	7
292	Confocal microscopy studies of shear-induced coalescence in blends of poly(butyl methacrylate) and poly(2-ethylhexyl methacrylate). Journal of Polymer Science, Part B: Polymer Physics, 2001, 39, 2317-2332.	2.1	7
293	Slow morphology evolution of block copolymer–quantum dot hybrid networks in solution. Soft Matter, 2013, 9, 8887.	2.7	7
294	Direct Synthesis of CdSe Nanocrystals with Electroactive Ligands. Chemistry of Materials, 2016, 28, 4953-4961.	6.7	7
295	EGFR-Targeted Metal Chelating Polymers (MCPs) Harboring Multiple Pendant PEG2K Chains for MicroPET/CT Imaging of Patient-Derived Pancreatic Cancer Xenografts. ACS Biomaterials Science and Engineering, 2017, 3, 279-290.	5.2	7
296	Monitoring Polymer Diffusion in a Waterborne 2K Polyurethane Formulation Based on an Acrylic Polyol Latex. Macromolecules, 2020, 53, 10744-10753.	4.8	7
297	Monte Carlo simulation of a lattice model of intramolecular exciplex formation. Journal of Chemical Physics, 1981, 75, 4683-4695.	3.0	6
298	Direct nonâ€radiative energy transfer studies of interdiffusion latex films: Strategies for data analysis. Macromolecular Symposia, 1995, 92, 321-331.	0.7	6
299	Synthesis and characterization of nonaqueous dispersion particles with photolabile ?-heptadecylphenacyl ester stabilizer chains. Journal of Polymer Science Part A, 2001, 39, 2642-2657.	2.3	6
300	Numerical Simulations of Fluorescence Resonance Energy Transfer in Diblock Copolymer Lamellae. Macromolecules, 2005, 38, 8882-8890.	4.8	6
301	Structure and Excitedâ€State Interactions in Composites of CdSe Nanorods and Interfaceâ€Compatible Polythiopheneâ€ <i>graft</i> â€poly( <i>N</i> , <i>N</i> â€dimethylaminoethyl methacrylates). Macromolecular Chemistry and Physics, 2010, 211, 393-403.	2.2	6
302	Form Factor of Asymmetric Elongated Micelles: Playing with Russian Dolls Has Never Been so Informative. Journal of Physical Chemistry B, 2014, 118, 10740-10749.	2.6	6
303	Urethane-Coupled Poly(ethylene glycol) Polymers Containing Hydrophobic End Groups. Advances in Chemistry Series, 1996, , 363-376.	0.6	5
304	Nanosize Lipophilic Polyacrylate Particles and Their Photoinduced Flocculation in Hydrocarbon Solvents. Journal of Physical Chemistry A, 1998, 102, 5349-5355.	2.5	5
305	Synthesis and spectroscopic characterization of symmetrical isoprene-methyl methacrylate diblock copolymers bearing different anthracene derivatives at the junctions. Journal of Polymer Science Part A, 2003, 41, 1225-1236.	2.3	5
306	Synthesis of dye-labeled poly(vinyl acetate-co-ethylene) (EVA) latex and polymer diffusion in their latex films. Journal of Polymer Science Part A, 2005, 43, 5581-5596.	2.3	5

#	Article	IF	CITATIONS
307	Kinetics of Two-Stage Dispersion Copolymerization for the Preparation of Lanthanide-Encoded Polystyrene Microparticles. Macromolecules, 2013, 46, 2523-2534.	4.8	5
308	Investigating Molecular Exchange between Partially Cross-Linked Polymer Particles Prepared by a Secondary Dispersion Process. Macromolecules, 2019, 52, 5245-5254.	4.8	5
309	Influence of the Sodium Precursor on the Cubic-to-Hexagonal Phase Transformation and Controlled Preparation of Uniform NaNdF <sub>4</sub> Nanoparticles. Langmuir, 2021, 37, 2146-2152.	3.5	5
310	Photocleavage of the acetate of a hydroxyphenyl benzotriazole UV absorber: The search for a photo-Fries rearrangement product. Journal of Polymer Science: Polymer Chemistry Edition, 1983, 21, 1263-1271.	0.8	4
311	Attachment of fluorescent dyes to polyacrylamides in aqueous media. Journal of Polymer Science Part A, 1990, 28, 2075-2083.	2.3	4
312	Energy transfer from phenanthrene to anthracene in a dye-labeled (ethylene-methyl acrylate) copolymer. Journal of Polymer Science Part A, 1999, 37, 4169-4175.	2.3	4
313	Gold-nanoparticle coated La, Tb-encoded PS beads and their application in investigating the performance of the inductively coupled plasma of a mass cytometer. Journal of Analytical Atomic Spectrometry, 2013, 28, 1475.	3.0	4
314	Spheruliteâ€Like Micelles. Angewandte Chemie, 2021, 133, 11045-11051.	2.0	4
315	Control of Metal Content in Polystyrene Microbeads Prepared with Metal Complexes of DTPA Derivatives. Chemistry of Materials, 2021, 33, 3802-3813.	6.7	4
316	A Silica Coating Approach to Enhance Bioconjugation on Metal-Encoded Polystyrene Microbeads for Bead-Based Assays in Mass Cytometry. Langmuir, 2021, 37, 8240-8252.	3.5	4
317	Influence of intraparticle cross-linking on polymer diffusion in latex films prepared from secondary dispersions. Progress in Organic Coatings, 2022, 164, 106691.	3.9	4
318	Influence of Polar Substituents at the Latex Surface on Polymer Interdiffusion Rates in Latex Films. ACS Symposium Series, 1996, , 51-63.	0.5	3
319	Contrast Inversion in TEM Studies of Poly(ferrocenylsilane)â€≺i>blockâ€Poly(dimethylsiloxane) Diblock Copolymers. Macromolecular Chemistry and Physics, 2008, 209, 1432-1436.	2.2	3
320	Effect of Excess Ligand on the Reverse Microemulsion Silica Coating of NaLnF <sub>4</sub> Nanoparticles. Langmuir, 2022, 38, 3316-3326.	3.5	3
321	Scratching the Surface (Modification): Developing a Quantitative Liquid Chromatography–Tandem Mass Spectrometry Method for the Investigation of PEGylated and Non-PEGylated Lipid Mixtures on Lipid-Coated Lanthanide Nanoparticles. Langmuir, 2021, 37, 14605-14613.	3.5	3
322	Solvent Concentration Profile of Poly(methyl methacrylate) Dissolving in Methyl Ethyl Ketone. ACS Symposium Series, 1989, , 385-399.	0.5	2
323	A new method to measure molecular weight dependence of intramolecular excimer formation in polymer solutions. Journal of Polymer Science, Part C: Polymer Letters, 1989, 27, 21-24.	0.7	2
324	The characterization of polymer interfaces by fluorescence decay measurements. Makromolekulare Chemie Macromolecular Symposia, 1992, 53, 327-343.	0.6	2

#	Article	IF	CITATIONS
325	Thermal decomposition behavior of naphthalene-labeled polyethylene. Journal of Polymer Science Part A, 1996, 34, 2045-2049.	2.3	2

326 Synthesis of an alkali-swellable emulsion and its effect on the rate of polymer diffusion in poly(vinyl) Tj ETQq0 0 0 rgBT /Overlock 10 Tf 5

327	Creating Biomorphic Barbed and Branched Mesostructures in Solution through Block Copolymer Crystallization. Angewandte Chemie, 2018, 130, 17451-17456.	2.0	2
328	Synthesis of a metal-chelating polymer with NOTA pendants as a carrier for 64Cu, intended for radioimmunotherapy. European Polymer Journal, 2020, 125, 109501.	5.4	2
329	Monitoring the reaction kinetics of waterborne 2â€pack polyurethane coatings in the dispersion and during film formation. Canadian Journal of Chemical Engineering, 2022, 100, 703-713.	1.7	2
330	Film Formation of Waterborne 2K Polyurethanes: Effect of Polyols Containing Different Carboxylic Acid Content. Macromolecules, 2021, 54, 7943-7954.	4.8	2
331	In-Depth Analysis of the Effect of Fragmentation on the Crystallization-Driven Self-Assembly Growth Kinetics of 1D Micelles Studied by Seed Trapping. Polymers, 2021, 13, 3122.	4.5	2
332	Biotinylated Lipid-Coated NaLnF <sub>4</sub> Nanoparticles: Demonstrating the Use of Lanthanide Nanoparticle-Based Reporters in Suspension and Imaging Mass Cytometry. Langmuir, 2022, 38, 2525-2537.	3.5	2
333	A discrete scattering series representation for lattice embedded models of chain cyclization. Journal of Chemical Physics, 1980, 72, 728-735.	3.0	1
334	Study of Complex Polymer Materials. ACS Symposium Series, 1987, , 8-17.	0.5	1
335	Interface Structure in a Polymer Blend in the Presence of Selective Solvents. Israel Journal of Chemistry, 1991, 31, 119-125.	2.3	1
336	In-line monitoring of immiscible polymer blends in a rheometer with a fiber-optics-assisted fluorescence detection system. Journal of Polymer Science, Part B: Polymer Physics, 2001, 39, 2302-2316.	2.1	1
337	Self-Assembly of Ferrocene-Based Block Copolymers: A Route to Supramolecular Organometallic Materials. ACS Symposium Series, 2002, , 149-162.	0.5	1
338	Synthesis and Solution Self-Assembly of Polyferrocene-Based AB Diblock and ABC Triblock Copolymers. , 2003, , 75-84.		1
339	Aqueous Metallosupramolecular Micelles with Spherical or Cylindrical Morphology. ACS Symposium Series, 2006, , 30-42.	0.5	1
340	Herbert Morawetz and the First Nonradiative Energy Transfer Studies of Miscibility in Polymer Blends. Macromolecules, 2020, 53, 1881-1883.	4.8	1
341	Synthesis, characterization, and stability of carbodiimide groups in carbodiimide-functionalized latex dispersions and films. Journal of Polymer Science Part A, 2000, 38, 855.	2.3	1
342	Synthesis and Aqueous Self-Assembly of a Polyferrocenylsilane-block-poly(aminoalkyl methacrylate) Diblock Copolymer. , 2002, 23, 210.		1

#	Article	IF	CITATIONS
343	Changing Surface Polyethylene Glycol Architecture Affects Elongated Nanoparticle Penetration into Multicellular Tumor Spheroids. Biomacromolecules, 2022, 23, 3296-3307.	5.4	1
344	Excluded Volume Effects on Polymer Cyclization. ACS Symposium Series, 1987, , 57-67.	0.5	0
345	Synthesis and Self-Assembly of Polyisoprene-Block -Polyferrocenyldimethylsilane Diblock Copolymers: Fabrication of Ceramic Nanolines on Semiconducting Substrates. , 2003, , 85-97.		0
346	Site-Specific Conjugation of Metal-Chelating Polymers to Anti-Frizzled-2 Antibodies via Microbial Transglutaminase. Biomacromolecules, 2021, 22, 2491-2504.	5.4	0
347	Synthesis, Self-Assembly and Applications of Polyferrocenylsilane (PFS) Block Copolymers. , 0, , 151-168.		0